

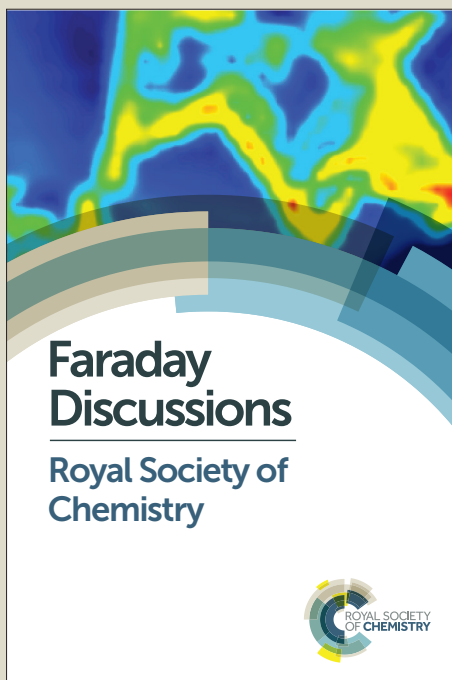
Faraday Discussions

Accepted Manuscript



This manuscript will be presented and discussed at a forthcoming Faraday Discussion meeting. All delegates can contribute to the discussion which will be included in the final volume.

Register now to attend! Full details of all upcoming meetings: <http://rsc.li/fd-upcoming-meetings>



This is an *Accepted Manuscript*, which has been through the Royal Society of Chemistry peer review process and has been accepted for publication.

Accepted Manuscripts are published online shortly after acceptance, before technical editing, formatting and proof reading. Using this free service, authors can make their results available to the community, in citable form, before we publish the edited article. We will replace this *Accepted Manuscript* with the edited and formatted *Advance Article* as soon as it is available.

You can find more information about *Accepted Manuscripts* in the [Information for Authors](#).

Please note that technical editing may introduce minor changes to the text and/or graphics, which may alter content. The journal's standard [Terms & Conditions](#) and the [Ethical guidelines](#) still apply. In no event shall the Royal Society of Chemistry be held responsible for any errors or omissions in this *Accepted Manuscript* or any consequences arising from the use of any information it contains.

Inkjet printing of graphene

Kirill Arapov*^a, Robert Abbel^b, Gijbertus de With^a and Heiner Friedrich^a

DOI: 10.1039/b000000x [DO NOT ALTER/DELETE THIS TEXT]

5 Inkjet printing of graphene is a cost-effective, and versatile deposition
technique for both transparent and non-transparent conductive films.
Printing graphene on paper is aiming for low-end, high-volume
applications, i.e., in electromagnetic shielding, photovoltaics or, e.g., as
replacement of metal in the antennas of radio-frequency identification
10 devices improving their recyclability and biocompatibility. Here, we
present a comparison of two graphene inks, one prepared by solubilization
of expanded graphite in the presence of a surface active polymer and the
other by covalent graphene functionalization followed by redispersion in a
solvent but without surfactant. The non-oxidative functionalization of
15 graphite in the form of a donor-type graphite intercalation compound is
carried out by a Birch-type alkylation, where graphene can be viewed as a
macrocarbanion. To increase the amount of functionalization we employed
a graphite precursor with a high edge to bulk carbon ratio, thus, allowing us
to achieve up to six weight percent of functional groups. The functionalized
20 graphene can be readily dispersed at concentrations of up to 3 mg/ml in
non-toxic organic solvents and is colloidally stable for more than 2 months.
The two inks are readily inkjet printable with good to satisfactory
spreading. Analysis of the sheet resistance of deposited films demonstrate
that inks based on expanded graphite outperform functionalized graphene
25 inks, possibly due to the significantly larger graphene sheet size in the
former, which minimizes the number of sheet-to-sheet contacts along the
conductive path. We found that the sheet resistance of printed large-area
films is decreasing with an increase of the number of printed layers.
Conductivity levels reach approximately 1-2 k Ω / \square for 15 printing passes
30 which roughly equals a film thickness of 800 nm for expanded graphite
based inks and 2 M Ω / \square for 15 printing passes of functionalized graphene
having a 900 nm film thickness. Our results show that ink preparation and
inkjet printing of graphene-based inks is simple and efficient, therefore has
a high potential to compete with other conductive ink formulations for
35 large-area printing of conductive films.

1 Introduction

Manufacturing of large-area graphene thin films is an important step towards
commercialization of graphene based technologies. Inkjet printing of graphene is
40 one method for the controlled deposition of large-area transparent or non-transparent
conductive films.¹⁻⁶ In comparison with other approaches such as chemical vapor
deposition (CVD)^{7, 8} inkjet printing is a poor competitor. This holds true especially

for transparent graphene thin films,^{1, 2} where high conductivity, high transparency together with precise control over the number of layers and defect density is required. Nevertheless, printing of graphene has a very high potential for applications, where non-transparent but highly conductive patterns are required.⁹ Examples of such low-end, high-volume applications could be radio frequency identification tags (RFID tag) or electromagnetic shielding, or devices where graphene printing of conductive patterns can be effectively utilized. Henceforth graphene inks made from graphite have the potential to revolutionize the field of printed conductors by replacing metallic inks while at the same time reducing biological hazards and production costs.

There are several reports on graphene-based inks encompassing different preparation routes including oxidation of graphite to graphite oxide,^{1, 2, 10-12} extended ultrasonication of graphite with^{3, 13} or without surfactant.⁶ The majority of studies on non-oxidized graphene report relatively low graphene concentration,^{2, 6} poor conductivity² and rather low ratio of graphene to surfactant.⁹ Recently, the successful non-oxidative functionalization of graphene was shown leading to slightly improved dispersibility in a number of solvents.¹⁴⁻¹⁶ Functionalization seems to be very promising for graphene inks as it allows to avoid the use of surfactants for colloidal stabilization, which in turn has been made responsible for decreasing the conductive properties of a printed layer by increasing the sheet-to-sheet contact resistance. Unfortunately, the demonstrated amount of graphene functionalization and, thus, product dispersibility, is far from ideal, a point which this paper will address.

In this paper we describe two methods for the preparation of graphene-based inks. First, a simple, efficient and up-scalable method is presented starting from raw graphite and avoiding any oxidation steps to preserve the conductive properties of the graphene throughout the entire process. Second, a non-oxidative covalent functionalization of graphene is presented resulting in a final product dispersibility up to 3 mg/ml in non-toxic solvents. Subsequently we studied the printability of the two inks using two paper substrates, namely FS3 and LumiForte special application papers which are widely used as substrates for inkjet and screen printing of conductive patterns. Furthermore, the performance of the two inks was evaluated by means of sheet resistance measurements of large printed areas as a function of the number of printed layers.

2 Experimental

2.1 Preparation of expanded graphite (EG) from Li(THF)GIC

Synthesis of the ternary graphite intercalation compound with Li in THF (Li-THF-GIC) was performed using the procedure of Nomine and Bonnetain.¹⁷ Briefly, 1.28 g of naphthalene C₈H₁₀ (0.01 mol, Alfa Aesar, USA) were dissolved in 100 ml of freshly distilled tetrahydrofuran (THF) by vigorous stirring followed by addition of 0.12 g of freshly cut metallic lithium (0.017 mol, Alfa Aesar, USA). Then 0.5 g of -10 mesh graphite (0.042 mol, Alfa Aesar, USA or Asbury Graphite, USA) were added to the reaction mixture at once. The reaction flask was then sealed and left stirring for another 72 hours. The Li-THF-GIC was separated from the side products by decantation followed by rinsing with freshly distilled THF. The residue was filtered and dried in ambient conditions for 20 minutes.

The freshly prepared GIC was placed at the bottom of a Vitreosil quartz crucible ensuring that all particles are in mutual contact. The crucible was placed in 2450 MHz 700 W home appliance microwave oven and exposed to irradiation for 1 minute. As prepared expanded graphite (EG) was used without any further treatment.

2.2 EG ink preparation with Plasdane S-630

EG (1.4 mg/ml) was added to a glass vial containing 5 mg/ml of 60:40 copolymer of N-vinyl-2-pyrrolidone and vinyl acetate (Plasdane S 630, Ashland Inc., USA) dissolved in a mixture of isopropanol (IPA) and n-butanol (n-BuOH) with volume ratio of 1:3. The slurry was ultrasonicated (Branson 1510DTH SB) in ice water for 30 minutes. The so obtained dispersion was used further without any treatment.

2.3 Functionalization of graphite platelet carbon nanofibers (GCNF)

The synthesis and functionalization of graphite via a potassium intercalation compound (C_8K GIC) were performed in N_2 glovebox with O_2 concentration < 0.1 ppm, $H_2O < 0.1$ ppm.

Preparation of NaK. Liquid NaK alloy was prepared similar to ref.¹⁸. Briefly, freshly cut and dry pieces of Na and K with a mass ratio of 1: 7.4 were pressed together and agitated with a spatula to obtain a liquid state alloy.

Preparation of C_8K GIC. Graphite platelet carbon nanofibers (100 mg, 0.0083 mol, Strem Chemicals, USA) were added to a 50 ml round bottom flask containing 20 ml of absolute THF and followed by an addition of 0.29 ml of freshly prepared NaK alloy. The reaction mass was stirred for 3 days to obtain a dark blue to green dispersion. Next, 0.9 g of *p*-nitrobenzylbromide (0.00416 mol, Merck Chemicals, Germany) were dissolved in 10 ml of absolute THF and added to a GIC dispersion by 0.5 ml every 1.5 hour. After addition the reaction mixture was additionally agitated for 1 day. Afterwards the sample was taken out of the glovebox, followed by quenching with isopropanol (5 ml), ethanol (5 ml), and finally water (5 ml). The reaction mass was then centrifuged at 8000 rpm for 30 minutes and the supernatant was discarded. The product was redispersed in THF:H₂O (3:1) mixture and centrifuged under the same conditions as described above. The washing procedure was repeated with the following solvent mixtures: IPA:H₂O (3:1), EtOH:H₂O (3:1), EtOH:H₂O (1:3), and H₂O. The washed product was finally redispersed in H₂O and filtered through 0.45 μ m pore size PTFE membrane and dried in vacuum at 50 °C to yield a black powder of *p*-nitrobenzyl functionalized graphite platelet carbon nanofiber (PNB-GCNF). This material was used for preparation of graphene inks without further treatment.

2.4 Ink preparation with PNB-GCNF

Powder of PNB-GCNF (3 mg/ml) was added to a vial containing propylene glycol diacetate (PGDA, The Dow Chemical Company, USA) and ultrasonicated (Branson 1510DTH SB) in ice water for 2.5 h. The as-prepared dispersion was used for printing without further treatments.

2.5 Printing conditions

Printing tests were performed on a Dimatix DMP 2800 system (Dimatix-Fujifilm Inc., USA), equipped with a 10 pl drop volume cartridge (DMC-11610). The print head contains 16 parallel squared nozzles with a diameter of 30 μm . The dispersion was printed at a voltage of 13 V, using a frequency of 5 kHz and a customized waveform. FS3 paper (Felix Schoeller, Germany) and LumiForte paper (Stora Enso, Finland) were used as substrates. The distance between printing head and substrate was set to 200 μm . The following patterns were printed: dots (3 lines, 200 μm drop spacing), rectangles of 5 \times 35 mm in size, and 3 pixel wide lines with 20 μm line distance. In the case of the functionalized graphene inks with propylene glycol diacetate as solvent, the substrate temperature was optimized to 50 $^{\circ}\text{C}$.

2.6 Thermal gravimetric analysis conditions

TGA measurements were performed using a TGA Q500 (TA Instruments, USA) in the temperature range 35–600 $^{\circ}\text{C}$ under N_2 gas flow with heating rate of 10 $^{\circ}\text{C min}^{-1}$.

2.7 X-ray photoelectron spectroscopy conditions

X-ray photoelectron spectroscopy (XPS) measurements were carried out with a K-Alpha, ThermoScientific spectrometer using an aluminum anode ($\text{Al K}\alpha = 1486.3$ eV) operating at 510 W with a background pressure of 8×10^{-8} mbar. The spectra were recorded using the VGX900 data system collecting 40 scans. The spectra were acquired at a take-off angle of 0° relative to the surface normal, corresponding to a probe depth of around 10 nm.

2.8 X-ray diffraction conditions

X-ray diffractograms were obtained on a Bragg-Brentano Rigaku Geigerflex diffractometer with $\text{CuK}\alpha$ irradiation using Lindemann capillaries with an internal diameter of 3 mm.

2.9 Sheet resistance measurement conditions

Sheet resistance was measured with a four-point probe setup (Source: Keithley 237 High Voltage Measure Unit, Resistance meter: Keithley 6517A High Resistance Meter) with an interprobe distance of 5 mm, in a range of currents from 10 nA to 1 mA.

3 Results and discussion

3.1 Preparation of ink with expanded graphite

The ink preparation workflow starts with a donor-type intercalation of raw graphite as shown in **Figure 1**. The donor-type intercalation compound (IC) is formed by donating electrons to the graphite matrix, thus, making it negatively charged and accompanied by the insertion of positively charged species to sandwich graphene layer between two layers of intercalants (Stage 1 IC).^{18, 19} In contrast to oxidation, i.e., the withdrawal of electrons from graphite matrix, such an approach prevents the formation of any functional groups, and hence, preserves the conductive properties of graphene. The formed stage 1 donor-type IC slowly decomposes upon exposure to ambient conditions into mixtures of higher stage IC.²⁰ For instance, the IC flake shown in Figure 1b exhibits charging effects at edges and planes which can be

attributed to lithium salts deintercalating from the graphite matrix. Therefore, intercalated materials were analyzed or used immediately after the synthesis.

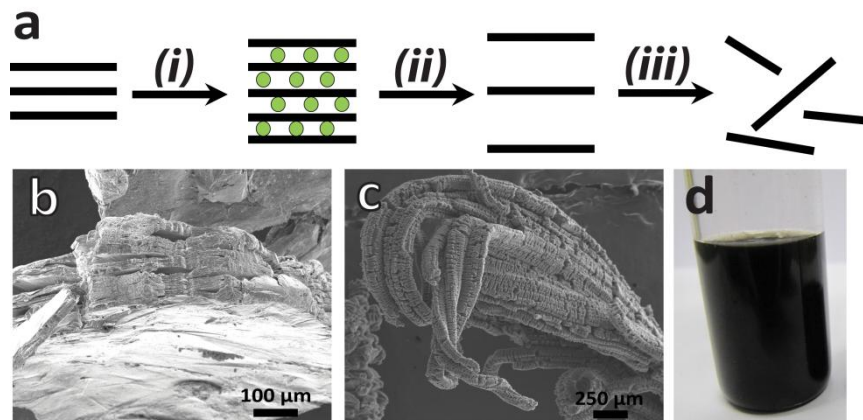


Figure 1. Preparation of graphene inks from raw graphite via intercalation. (a) Overall scheme showing: (i) graphite intercalation, (ii) thermal expansion, and (iii) liquid phase exfoliation; (b) Scanning electron micrograph of Li(THF) graphite intercalation compound; (c) Scanning electron micrograph of expanded graphite; (d) Graphene dispersion with concentration of 1.4 mg/ml prepared from expanded graphite.

10

To increase the distance between graphene layers and to promote layer separation the IC was subjected to high-speed thermal expansion by means of microwave irradiation. Rapid heating of the GIC results in an abrupt conversion of the intercalated species into the gas phase, thus, causing expansion of graphite planes along the *c*-axis.^{21, 22} The resulting expanded graphite (EG) has a porous worm-like structure, as shown in Figure 1c, with a significantly increased specific volume (more than 300 times as compared to initial IC). In the next step, EG with concentrations of up to 1.4 mg/ml was dispersed in a mixture of *i*-propanol and *n*-butanol to obtain a colloiddally stable dispersion (Figure 1d). For ink formulation we opted for the highest graphene content vs a reasonable colloiddal stability. We found experimentally that at a graphene concentration of 1.4 mg/ml against 5 mg/ml of surfactant the ink is colloiddally stable for more than 9 month, meanwhile providing a maximum graphene to surfactant ratio.

20

3.2 Preparation of ink with functionalized graphene

As an alternative to surfactant-based graphene ink formulation we developed a functionalized graphene ink (Figure 2a). To date, there are several studies on graphene functionalization^{14, 16, 23, 24} based on the chemistry of donor-type graphite intercalation compounds. Nevertheless, most approaches demonstrate only a very low amount of functionalization (thus poor dispersibility), which is in good agreement with the early works of Bergbreiter and Killough.²⁵ According to reference 25 in a donor-type IC the reactivities of edge and bulk carbon atoms are different, with the edge atoms undergoing the desired two-electron Birch-type alkylation, while bulk carbon just give up an electron via single electron transfer, thus acting as a catalyst for the undesired Wurtz-type coupling. This has led to the

35

conclusion that the edge-to-plane ratio of carbon atoms plays a significant role for functionalization efficiency. Therefore, instead of commonly used micrometer-sized graphite which has a low edge-to-plane carbon ratio, we used platelet-type, i.e. graphitic, carbon nanofibers (GCNF). This type of graphite with graphene sheet sizes of only 10-60 nm assures a high edge-to-plane carbon ratio (Figure 2b).

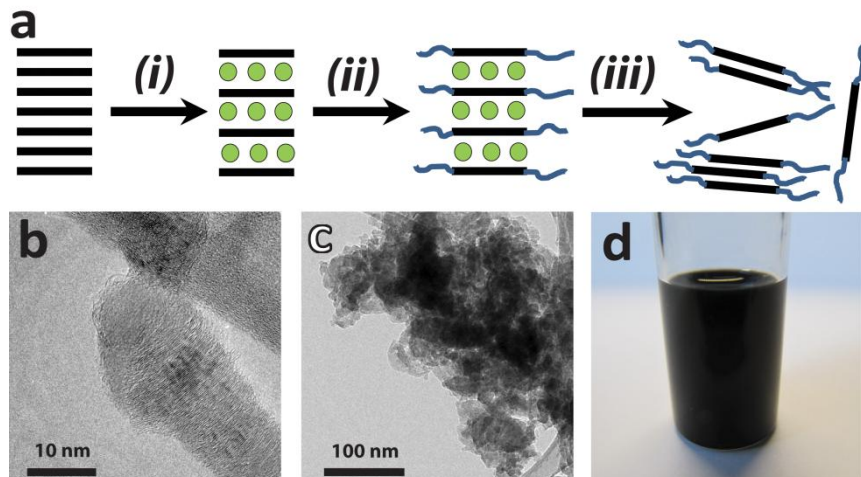


Figure 2. Preparation of functionalized graphene inks from graphitic carbon nanofibers (GCNF). (a) Scheme of GCNF functionalization (i) preparation of potassium-GCNF IC, (ii) functionalization of potassium-GCNF IC with *p*-nitrobenzyl bromide, and (iii) liquid phase exfoliation; (b) Transmission electron micrograph of starting GCNF; (c) Transmission electron micrograph of cast-dried functionalized GCNF; (d) PNB-GCNF dispersion with concentration of 3 mg/ml in propylene glycol diacetate.

According to the above concept, a high degree of functionalization can significantly improve the dispersibility of small sheet graphene due to an increased number of interaction sites between functional groups and solvent associates. Thus, we synthesized a potassium graphite intercalation compound with GCNF as a starting material for further functionalization. Next, we functionalized the so-obtained GCNF IC with *p*-nitrobenzyl bromide using an approach similar to the one described by Garst, Barbas, and Barton.²⁶ In order to minimize the formation of undesired Wurtz-type dimerization side products the concentration of alkyl radicals in solution had to be kept much lower than the concentration of the substrate. Such conditions can be achieved by slow alkylhalide vapour diffusion into the reaction medium or, as utilized in our procedure, by stepwise addition of a very dilute (see Experimental) alkylhalide solution. Upon addition of alkylhalide we observed significant volume expansion of the graphite phase indicating *in situ* exfoliation. The dried reaction product was found to be well dispersible in a number of solvents including ethanol, *i*-propanol, chlorinated solvents and some others. Transmission electron microscopy of a cast dried dispersion revealed that most of the GCNF fibers were exfoliated into platelets which were prone to agglomeration, as shown in Figure 2c.

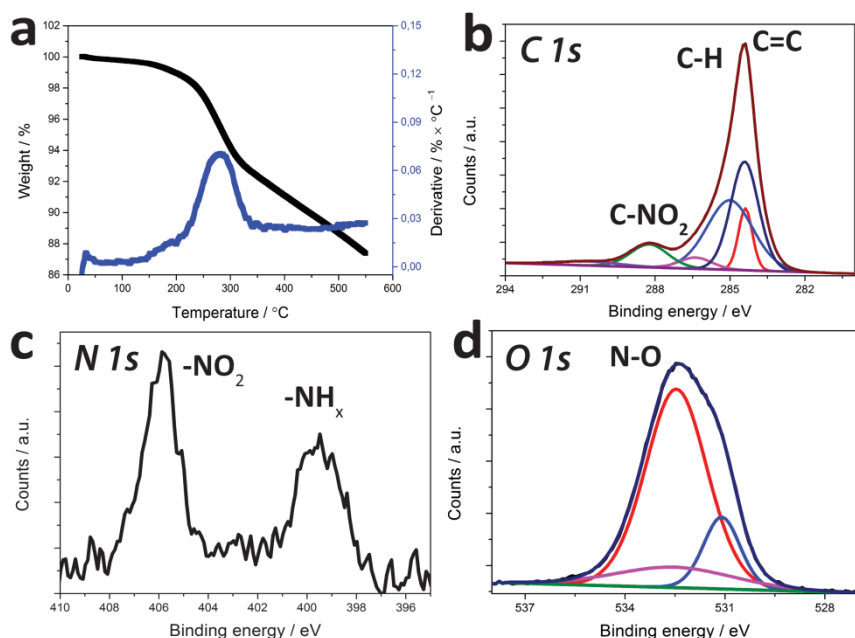


Figure 3. Analysis of *p*-nitrobenzyl functionalized carbon nanofibers. (a) Thermal gravimetric analysis in dry N₂ with heating rate 10 °C / min.; X-ray photoelectron spectra of (b) C 1s; (c) N 1s; (d) O 1s.

5

Further, we performed dispersibility tests in order to find an appropriate solvent for inkjet printing. Our criteria for the final formulation included non-toxicity of the solvent combined with a high solid content vs colloidal stability, and printability. Experimentally we found that an optimal solvent for *p*-nitrobenzyl functionalized GCNF (PNB-GCNF) is propylene glycol diacetate (PGDA) allowing a solid content of 3 mg/ml without the use of surfactants (Figure 2d). PGDA is a common solvent used for inkjet printing having a viscosity of 2.6 mPa×s (at 25 °C) and a surface tension of 32.9 mN/m (at 20 °C). The downside of this solvent is the rather low relative evaporation rate of 0.04 (*n*-butyl acetate = 1.0), which might extend the drying process.

15

3.3 Analysis of functionalized graphene

The functionalized GCNF graphene was subjected to thermal gravimetric analysis (TGA). In an inert atmosphere this technique revealed (Figure 3a) a sharp decomposition peak amounting by about 6 weight percent, which was attributed to the presence of functional groups (*p*-nitrobenzyl) of approximately one per 166 carbon atoms. This hypothesis was supported by X-ray photoelectron spectroscopy (Figure 3b-d). Here, XPS analysis confirmed the presence of carbon covalently bonded to a strong electron withdrawing group, i.e., C-NO₂ (Figure 3b).^{27, 28} Further, XPS showed the presence of nitrogen, presumably in a nitro group (-NO₂) as well as in reduced form -NH_x (possibly including hydroxylamine form), which can be explained by partial reduction of nitro groups by the NaK alloy (Figure 3c).^{28, 29} Also XPS spectra of oxygen show the presence of strong electron withdrawing

25

oxygen containing group such as $-\text{NO}_2$.²⁸ Quantification of XPS data by peak area adjusted with relative sensitivity factors³⁰ gave a relative carbon to nitrogen ratio of approximately 99 to 1. This corresponds to the functionalization degree of one *p*-nitrobenzyl group per 92 carbon atoms or theoretically 11 wt.%. The observed discrepancy between TGA and XPS data can be attributed to several factors such as probing depth, and sample surface roughness of the latter. Nevertheless, the results found by both techniques are comparable when the margin of errors are taken into account. Considering all the above results combined with the significantly improved dispersibility of the final product we concluded that functionalization had been successful.

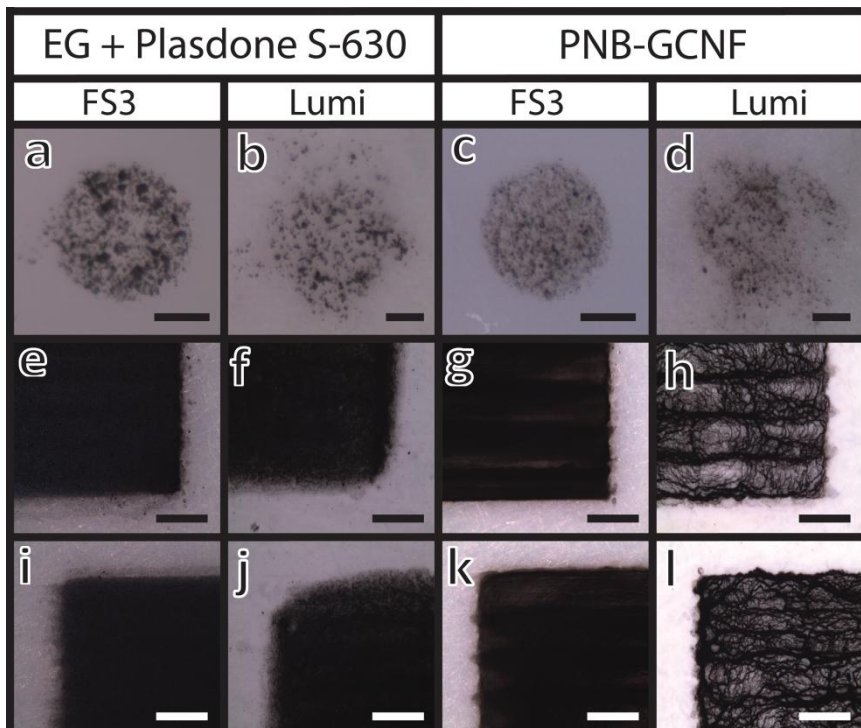


Figure 4. Graphene based inks printed on (a, e, i and c, g, k) – FS3 and (b, f, j and d, h, l) - Lumi papers. Expanded graphite with Plasdone S-630 (a and b) – dot, (e, i and f, j) – large-area rectangle, 10 printing passes. *p*-Nitrobenzyl functionalized graphene (c and d) – dot, (g, k and h, l) – large-area rectangle, 10 printing passes. Scale bars: (a-d) – 20 μm , (e-l) – 500 μm .

3.4 Inkjet printing of graphene-based inks onto paper substrates

Printing tests of the developed inks were performed on commercially available paper substrates, namely FS3 and Lumi. FS3 is a glossy, polymer-coated paper and Lumi is a matt and rougher paper. The presence of a polymer coating on FS3 minimizes the surface roughness, making it similar to polymeric foil substrates such as polyethylene terephthalate (PET), and it improves the adhesion of printed layers. Nevertheless, even with a coating on top FS3 still maintained its absorbing

properties towards solvents, and quickly separates the non-soluble components from soluble ones.

To analyze the spreading behavior of the inks, arrays of dots were printed. In Figure 4a-d optical micrographs of the corresponding shapes of printed dots are shown. It can be clearly seen that, independent from the ink formulation, the two substrates have different spreading behavior. Dots printed on FS3 paper have a round shape with sharp edges and no significant signs of “coffee stain” effects are observed. Contrary to FS3, both inks printed on Lumi paper demonstrate extensive spreading with an increase in dot size. In addition, printed dots have irregular shapes with ill-defined edges, thus significantly lowering the resolution of the printed features. All the above indicates clearly that independent from the ink formulation, both substrates have different spreading properties, with FS3 paper suppressing an expansion of the droplet while it is drying and adsorbing, whereas on Lumi paper the droplet is spreading while it is drying or being absorbed.

An important characteristic of evaluating ink-substrate compatibility is the edge resolution and the ink spreading over large printing areas. To this end, rectangles of 5×35 mm in size were printed with 1, 5, 10 and 15 printing passes on both paper substrates. In Figure 4e-l optical micrographs of the corners of the printed rectangles are presented. The corners of the rectangles printed on FS3 paper (Figures 4e, 4g, 4i, 4k) have sharp edges in the printing direction and perpendicular to it, demonstrating a fair printing definition. In the case of EG + Plasdone S-630 inks printed on Lumi paper (Figure 4f and 4j) it can be seen that the corners are rounded, which can be explained by the extensive spreading of the ink over the substrate. Overall the ink covered the substrate uniformly. Optical micrographs of functionalized graphene inks printed on Lumi paper (Figures 4h and 4l) also demonstrate a reasonable printing resolution with a distinct edge roughness, probably caused by the slow solvent evaporation and an increase of the Marangoni flow within a layer.

We found that ink spreading depends not only on substrate but also on the ink characteristics. Formulations based on expanded graphite with polymeric surfactant printed on FS3 substrate (Figure 4e and 4i) demonstrate good spreading and uniform particle distribution. This ink was formulated with a solvent mixture of highly volatile *i*-propanol and *n*-butanol, that evaporates quickly (evaporation rate of *i*-propanol = 2.9, *n*-butanol = 0.4, *n*-butyl acetate = 1.0), thus, minimizing any particle segregation and producing a homogeneous layer. For the same ink a similar behavior was observed in the case of Lumi paper (Figure 4f and 4j), where the ink spreads rather uniformly with minimal drying artefacts. Ink formulations based on functionalized graphene (PNB-GCNF) printed on FS3 paper (Figure 4g and 4k) demonstrate a non-uniform though regular particle segregation into lines parallel to the printing direction. This behavior is most likely caused by the slowly evaporating solvent and the ink's instability for locally high concentrations. This creates a pattern where lines of segregated material are poorly connected with each other, potentially causing anisotropy of the conductive properties. Spreading of the PNB-GCNF ink on the Lumi substrate (Figure 4h and 4l) is very complex with particle segregation not only along the printing direction but also perpendicular to it. This demonstrates that extensive spreading in combination with slow drying decreases printing resolution and overall printing quality.

3.5 Sheet resistance evaluation of inkjet graphene printed films on paper substrates

Along with the printability of inks, another highly important characteristic is the conductivity of the printed layers. We performed four point probe sheet resistance measurements of printed large-area rectangles with different numbers of layers, i.e., 1, 5, 10 and 15 printing passes. We found that in all cases single-pass printed rectangles are not conductive, indicating that the achieved coverage of conductive particles was below the percolation threshold. However, after subsequent printing passes a significant increase in conductivity of the printed layers was observed (Figure 5).

10

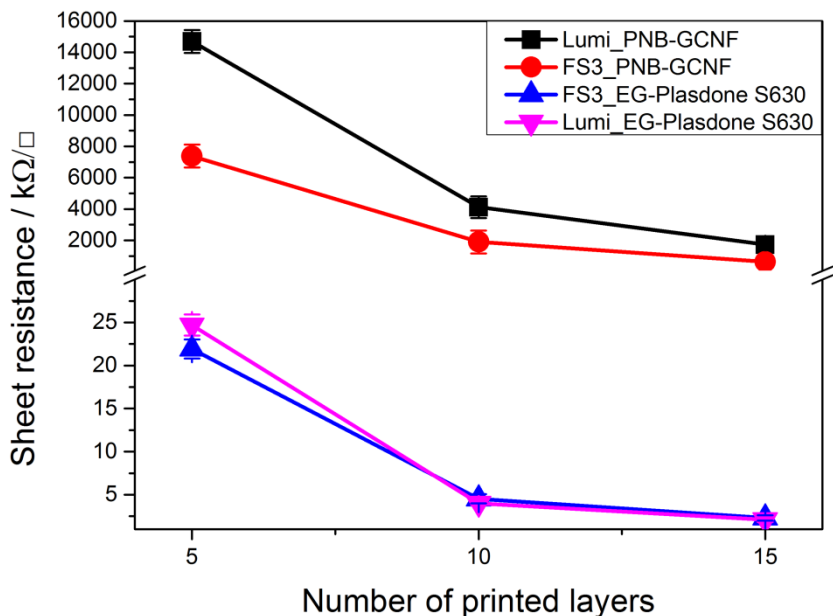


Figure 5. Sheet resistance of printed 5×35 mm rectangles as a function of number of printing passes.

15 We observed a significantly lower sheet resistance (R_s) for the ink prepared from expanded graphite and polymeric stabilizer than for the functionalized graphene based inks. As it can be seen from Figure 5, the trend is continued with an increase in a film sheet resistance of approximately 1-2 $k\Omega/\square$ for EG+Plasdone S-630 ink (800 nm thickness) and ~ 2 $M\Omega/\square$ for the PNB-GCNF ink (900 nm thickness).
 20 Remarkably, in the case of EG with Plasdone S-630 we did not notice any significant difference in R_s for the two paper substrates, which is in good agreement with the observed spreading of the ink (Figures 4e, 4i and 4f, 4j). However, we found a significant (~ 2 times) difference in R_s for the PNB-GCNF ink, which
 25 correlates with a difference in spreading and drying of the ink (Figures 4g, 4k and 4h, 4l) described earlier. Thus, inkjet printed films with uniform material distribution demonstrate lower and isotropic sheet resistance whilst printed films with non-uniform particle distribution show higher and anisotropic sheet resistance. From the observed sheet resistance data we hypothesize that the size of graphene

sheets plays a role in the conductive properties. If we assume that R_s of a graphene film scales with the resistance of the contact between two flakes ($R(\text{CR})$) and the resistance of graphene flake itself ($R(\text{GF})$), the number of contacts would give a major contribution to overall resistance. Here we assume that R_s for a flake is approximately constant for all sizes as it depends only on the defect density,³¹⁻³³ doping,³⁴⁻⁴⁰ etc. Since large (90% of population > 1 μm) graphene flakes of EG + Plasdone S-630 assemble into a layer with less contacts between each other compared to a layer of PNB-GCNF graphene (90 % of population < 60 nm), the overall sheet resistance of the former film (on both substrates) is much lower than that of the latter.

4 Conclusions

In this paper we demonstrate two approaches for graphene ink formulation: first, based on solubilization of graphene with a surface active polymer, and, second, based on covalent graphene functionalization. In the first route, we used a donor-type graphite intercalation compound as an intermediate prior to thermal expansion to avoid any oxidation of the graphene. We experimentally found that the presence of surface active polymer (60:40 copolymer of N-vinyl-2-pyrrolidone and vinyl acetate, Plasdone S-630) facilitates efficient graphene exfoliation allowing stable colloidal dispersions with concentrations of up to 1.4 mg/ml at polymer concentration of 5 mg/ml in a mixture of non-toxic solvents. The formulated ink is printable on any substrate including plastic foils and paper.

In the second route, we synthesized a potassium graphite intercalation compound with graphitic carbon nanofibers as a precursor and utilized it as an intermediate for covalent functionalization. We confirmed the hypothesis that high ratios between edge and bulk carbon atoms would increase Birch-type alkylation efficiency with *p*-nitrobenzylbromide, allowing up to six weight percent of functional moieties. The functionalized graphene is readily dispersible in a number of solvents at high concentrations including alcohols, ethers, and chlorinated solvents. We found that the optimal solvent is propylene glycol diacetate, which can disperse up to 3 mg/ml of solid material with a colloidal stability up to several months.

Both inks are printable on FS3 and Lumi paper substrates with good to satisfactory spreading. From our observations of spreading and drying behavior we concluded that the optimal combination is an ink of expanded graphite with Plasdone S-630 printed on FS3 paper as the ink forms a uniform layer with a reasonable print resolution. Further, we analyzed the conductive properties of the inks by measuring the sheet resistance of large-area printed rectangles. The evaluation of sheet resistance as a function of a number of printing passes showed a significant (up to 2000 times) difference between the two inks in favor of the one with expanded graphite. We hypothesize that this difference could be due to a much smaller number of sheet-to-sheet contacts and the overall resistance mainly depends on the resistance of graphene itself. In contrast to that, for a functionalized graphene printed film the number of sheet-to-sheet contacts is much larger, therefore, resistance of the film is limited by interlayer contact resistance. Such a hypothesis is a task for further investigation. Finally, we found that the sheet resistance is decreasing with an increase of the number of printing passes, providing the opportunity that further increase of the printed layer thickness can lower sheet

resistance to reach the conduction values achieved by metal based inks. Taking into account the simplicity and cost-effectiveness of our method, we believe that inkjet printing of graphene based inks is a good alternative for mass production of conductive films and devices on paper.

5

Acknowledgements

The research leading to these results has received funding from the European Union Seventh Framework Programme (FP7-MC-ITN) under grant agreement No. 264710. The authors would like to thank the Directorate-General for Science, Research and

10 Development of the European Commission for financial support of the research.

Authors would like to acknowledge Corne Rentrop (TNO, Eindhoven, The Netherlands) for providing paper for the experiment and valuable comments to the final version of the manuscript.

References

^a - Laboratory of Materials and Interface Chemistry, Dept. of Chemical Engineering and Chemistry, Eindhoven University of Technology, Den Dolech 2, 5612AZ, Eindhoven, The Netherlands
E-mail: h.friedrich@tue.nl

^b - Holst Centre – TNO, High Tech Campus 31, 5656AE, Eindhoven, The Netherlands
E-mail: robert.abbel@mo.nl

1. L. Huang, Y. Huang, J. Liang, X. Wan and Y. Chen, *Nano Research*, 2011, **4**, 675-684.
2. J. Li, F. Ye, S. Vaziri, M. Muhammed, M. C. Lemme and M. Ostling, *Adv Mater*, 2013, **25**, 3985-3992.
3. S. Lim, B. Kang, D. Kwak, W. H. Lee, J. A. Lim and K. Cho, *J. Phys. Chem. C*, 2012, **116**, 7520-7525.
4. E. B. Secor, P. L. Prabhurashi, K. Puntambekar, M. L. Geier and M. C. Hersam, *J. of Phys. Chem. Lett.*, 2013, **4**, 1347-1351.
5. Y. Su, J. Du, D. Sun, C. Liu and H. Cheng, *Nano Research*, 2013, **6**, 842-852.
6. F. Torrisi, T. Hasan, W. Wu, Z. Sun, A. Lombardo, T. S. Kulmala, G. W. Hsieh, S. Jung, F. Bonaccorso, P. J. Paul, D. Chu and A. C. Ferrari, *ACS Nano*, 2012, **6**, 2992-3006.
7. X. Li, Y. Zhu, W. Cai, M. Borysiak, B. Han, D. Chen, R. D. Piner, L. Colombo and R. S. Ruoff, *Nano Lett.*, 2009, **9**, 4359-4363.
8. A. Reina, X. Jia, J. Ho, D. Nezich, H. Son, V. Bulovic, M. S. Dresselhaus and J. Kong, *Nano Lett.*, 2009, **9**, 30-35.
9. *USA Pat.*, # 8,278,757, 2012.
10. V. Dua, S. P. Surwade, S. Ammu, S. R. Agnihotra, S. Jain, K. E. Roberts, S. Park, R. S. Ruoff and S. K. Manohar, *Angew Chem Int Ed Engl*, 2010, **49**, 2154-2157.
11. L. T. Le, M. H. Ervin, H. Qiu, B. E. Fuchs and W. Y. Lee, *Electrochem Commun*, 2011, **13**, 355-358.
12. L. T. Le, M. H. Ervin, H. Qiu, B. E. Fuchs, J. Zunino and W. Y. Lee, IEEE NANO 2011, Portland, OR, 2011.

13. H. Zhang, A. Xie, Y. Shen, L. Qiu and X. Tian, *Phys Chem Chem Phys*, 2012, **14**, 12757-12763.
14. J. M. Englert, K. C. Knirsch, C. Dotzer, B. Butz, F. Hauke, E. Spiecker and A. Hirsch, *Chem Commun (Camb)*, 2012, **48**, 5025-5027.
- 5 15. L. H. Liu, M. M. Lerner and M. Yan, *Nano Lett*, 2010, **10**, 3754-3756.
16. B. Genorio, W. Lu, A. M. Dimiev, Y. Zhu, A. R. Raji, B. Novosel, L. B. Alemany and J. M. Tour, *ACS Nano*, 2012, **6**, 4231-4240.
17. M. Nomine, Bonnetain, L., *J. Chim. Phys.*, 1969, **66**, 1731-1741.
18. L. M. Viculis, J. J. Mack, O. M. Mayer, H. T. Hahn and R. B. Kaner, *Journal of Materials Chemistry*, 2005, **15**, 974.
- 10 19. M. S. Dresselhaus and G. Dresselhaus, *Advances in Physics*, 2002, **51**, 1-186.
20. M. Inagaki and O. Tanaike, *Carbon*, 2001, **39**, 1083-1090.
21. Y. W. Zhu, S. Murali, M. D. Stoller, A. Velamakanni, R. D. Piner and R. S. Ruoff, *Carbon*, 2010, **48**, 2118-2122.
- 15 22. S. Jin, L.-s. Xie, Y.-l. Ma, J.-j. Han, Z. Xia, G.-x. Zhang, S.-m. Dong and Y.-y. Wang, *Journal of Physics: Conference Series*, 2009, **188**, 012040.
23. S. Chakraborty, J. Chattopadhyay, W. Guo and W. E. Billups, *Angew. Chem. Int. Ed. Engl.*, 2007, **46**, 4486-4488.
24. J. M. Englert, C. Dotzer, G. Yang, M. Schmid, C. Papp, J. M. Gottfried, H. P. Steinruck, E. Spiecker, F. Hauke and A. Hirsch, *Nat Chem*, 2011, **3**, 279-286.
- 20 25. D. E. Bergbreiter and J. M. Killough, *J Am Chem Soc*, 1978, **100**, 2126-2134.
26. J. F. Garst, J. T. Barbas and F. E. Barton, *J Am Chem Soc*, 1968, **90**, 7159-7160.
27. E. Bekyarova, S. Sarkar, S. Niyogi, M. E. Itkis and R. C. Haddon, *Journal of Physics D: Applied Physics*, 2012, **45**, 154009.
- 25 28. A. K. Haridas, C. S. Sharma, V. Sriharan and T. N. Rao, *RSC Advances*, 2014, **4**, 12188.
29. G. Yang, H. Hu, Y. Zhou, Y. Hu, H. Huang, F. Nie and W. Shi, *Sci Rep*, 2012, **2**, 698.
30. C. D. Wagner, L. E. Davis, M. V. Zeller, J. A. Taylor, R. H. Raymond and L. H. Gale, *Surface and Interface Analysis*, 1981, **3**, 211-225.
31. J.-H. Chen, W. Cullen, C. Jang, M. Fuhrer and E. Williams, *Phys Rev Lett*, 2009, **102**.
- 30 32. K. W. Clark, X. G. Zhang, I. V. Vlasiouk, G. He, R. M. Feenstra and A. P. Li, *ACS Nano*, 2013, **7**, 7956-7966.
33. A. Lherbier, S. M. M. Dubois, X. Declerck, S. Roche, Y.-M. Niquet and J.-C. Charlier, *Phys Rev Lett*, 2011, **106**.
34. A. Benayad, H. J. Shin, H. K. Park, S. M. Yoon, K. K. Kim, M. H. Jin, H. K. Jeong, J. C. Lee, J. Y. Choi and Y. H. Lee, *Chem. Phys. Lett.*, 2009, **475**, 91-95.
- 35 35. A. Kasry, M. A. Kuroda, G. J. Martyna, G. S. Tulevski and A. A. Bol, *ACS Nano*, 2010, **4**, 3839-3844.
36. K. K. Kim, A. Reina, Y. Shi, H. Park, L. J. Li, Y. H. Lee and J. Kong, *Nanotechnology*, 2010, **21**, 285205.
- 40 37. T. Kobayashi, M. Bando, N. Kimura, K. Shimizu, K. Kadono, N. Umezu, K. Miyahara, S. Hayazaki, S. Nagai, Y. Mizuguchi, Y. Murakami and D. Hobara, *Appl. Phys. Lett.*, 2013, **102**, 023112.
38. H. Mousavi and R. Moradian, *Solid State Sciences*, 2011, **13**, 1459-1464.
39. Y. J. Ren, S. S. Chen, W. W. Cai, Y. W. Zhu, C. F. Zhu and R. S. Ruoff, *Appl. Phys. Lett.*, 2010, **97**, 053107.
- 45 40. S. Tongay, K. Berke, M. Lemaitre, Z. Nasrollahi, D. B. Tanner, A. F. Hebard and B. R. Appleton, *Nanotechnology*, 2011, **22**, 425701.